The Journal of Chemical Physics

RAPID COMMUNICATION | AUGUST 19 2025

Interaction strength of carbon dioxide on graphene from periodic quantum diffusion Monte Carlo

Flaviano Della Pia ; Giaan Kler-Young ; Andrea Zen ; Fabian Berger ; Dario Alfè ; Angelos Michaelides

J. Chem. Phys. 163, 071101 (2025)
https://doi.org/10.1063/5.0283254

The Journal of Chemical Physics

COMMUNICATION

pubs.aip.org/aip/jcp

Interaction strength of carbon dioxide on graphene from periodic quantum diffusion Monte Carlo

Cite as: J. Chem. Phys. 163, 071101 (2025); doi: 10.1063/5.0283254
Submitted: 30 May 2025 • Accepted: 24 July 2025 •
Published Online: 19 August 2025

View Online Export Citation CrossMark

Flaviano Della Pia,[1] Giaan Kler-Young,[1] Andrea Zen,[2,3] Fabian Berger,[1] Dario Alfè,[2,3,4] and Angelos Michaelides[1,a)]

AFFILIATIONS

[1] Yusuf Hamied Department of Chemistry, University of Cambridge, Cambridge CB2 1EW, United Kingdom
[2] Dipartimento di Fisica Ettore Pancini, Università di Napoli Federico II, Monte S. Angelo, I-80126 Napoli, Italy
[3] Department of Earth Sciences, University College London, London WC1E 6BT, United Kingdom
[4] Thomas Young Centre and London Centre for Nanotechnology, University College London, London WC1E 6BT, United Kingdom

[a)] **Author to whom correspondence should be addressed:** am452@cam.ac.uk

ABSTRACT

Despite the importance of graphene based carbon capture devices, an accurate estimate of the interaction strength of a carbon dioxide molecule with graphene from periodic calculations is lacking. In this work, we compute a fixed node quantum diffusion Monte Carlo reference value for the interaction energy of a carbon dioxide molecule with a periodic free-standing graphene sheet, obtaining a value of -152 ± 15 meV. In addition, we evaluate the performance of several widely used density functional theory approximations and foundation machine learning interatomic potentials, for both carbon dioxide and water adsorption on graphene, competitive processes that play an important role in carbon capture technologies. Among the approaches tested, the B86bPBE-XDM, PBE-D3, revPBE-D3, rev-vdW-DF2, SCAN+rVV10, and PBE0-D3-ATM functionals achieve the closest agreement with DMC for the carbon dioxide–graphene interaction. The vdW-DF2, rev-vdW-DF2, and PBE0-D4-ATM functionals perform better for the competitive adsorption of water and carbon dioxide.

Nanoporous carbon-based devices are becoming increasingly popular for energy storage applications,[1,2] chemical sensors,[3–7] and carbon dioxide capture strategies.[8–13] However, a fundamental question at the base of any CO_2–graphene-based device remains unanswered: what is the interaction strength of a CO_2 molecule with a graphene sheet?

Recent experiments analyzed the adsorption of carbon dioxide on epitaxial graphene.[14,15] In particular, Takeuchi *et al.*[14] measured an adsorption energy of carbon dioxide on a monolayer of epitaxial graphene on a SiC(0001) surface of ~312 ± 15 meV at low CO_2 coverage ($\theta = 0.02$, where θ is the ratio between the number of CO_2 molecules and the number of carbon atoms in the graphene layer), which decreased to 263 ± 15 meV at higher coverages ($\theta = 0.08$). In addition to the experiment, using periodic density functional theory (DFT), they suggested that CO_2 is adsorbed parallel to the surface. Smith and Kay[15] measured an adsorption energy of ~270 ± 21 meV for low CO_2 coverage on a graphene sheet attached to a Pt(111) substrate, although they suggest that CO_2 is tilted away from the surface rather than parallel. These measurements imply that the underlying substrate has a significant influence on both the adsorption energy and adsorption structure; making a well-defined determination of the adsorption energy on a free-standing graphene sheet desirable.

Simulations, therefore, provide an important tool to obtain the necessary atomistic resolution and gain insight into the physicochemical processes at the heart of these devices. Unfortunately, calculations with DFT—the workhorse of materials science—yield a large range of values for the CO_2–graphene interaction energy. In particular, the interaction energy depends sensitively on the exchange–correlation functional used, varying in a range larger than 200 meV.[14,16] In this context, providing reference data for the interaction energy is crucial to inform the choice of the DFT approximation, or the parameterization of classical or machine learning

force fields, to be employed in large-scale routine simulations of carbon-based devices.

In principle, high accuracy quantum mechanical methods provide a route to accurate reference data.[16–18] In fact, a recent *tour de force* involving both periodic DFT, as well as coupled cluster with single, double, and perturbative triple excitations, and symmetry adapted perturbation theory (SAPT) calculations with cluster models, suggested that CO_2 is adsorbed parallel to the surface and that the adsorption energy can change by ~30 meV between free-standing and supported graphene.[16] Despite the valuable insight into the adsorption process of carbon dioxide on graphene that these calculations provided, explicit periodic calculations with quantum chemistry accuracy for the interaction energy of carbon dioxide on graphene are still missing.

In this brief Communication, we report the interaction energy curve for the CO_2 molecule on graphene using periodic fixed node quantum diffusion Monte Carlo (FN-DMC), a widely trusted approach for the description of interaction energies of molecules on surfaces,[17,19–29] as well as in gas and condensed phases.[30–35] In particular, we obtain an interaction energy of -152 ± 15 meV at a CO_2–graphene distance of ~ 3.24 Å. In addition, we compute the interaction energy curves with several widely used DFT approximations, as well as recent foundation machine-learning interatomic potentials (MLIPs). Finally, we benchmark the performance of both the DFT functionals and the MLIPs on the difference between the interaction energy of carbon dioxide and water on graphene, whose competitive adsorption plays a fundamental role in carbon capture technologies, such as supercapacitors,[12,13,36] metal–organic frameworks,[37–39] and more. Overall, the reference FN-DMC values allow us to identify reliable approximations to be used for the description of the carbon dioxide–graphene and water–graphene interactions and can be used as useful reference data to benchmark additional approximations and to parameterize analytical potentials.

To compute the interaction energy of the CO_2 molecule on a periodic graphene layer, we use an established approach that has been used before for FN-DMC adsorption energy calculations on similar systems, such as water or hydrogen molecules adsorbed on graphene[20,21] and hBN.[20] This approach consists of estimating the interaction energy as

$$E_{\text{int}} = E_{\text{b}} - E_{\text{f}}, \tag{1}$$

where E_{b} is the total energy of the bound configuration, i.e., the configuration with the CO_2 molecule adsorbed on the graphene layer, and E_{f} is the total energy of the configuration with the CO_2 molecule far from the substrate, at a distance of ~ 10 Å. The CO_2–graphene distance is evaluated as the distance between the carbon atom in the carbon dioxide molecule and the flat graphene sheet. We use a 5×5 graphene supercell with a 25 Å vacuum in the direction perpendicular to the graphene sheet. The initial adsorption structure, corresponding to the "bridge" carbon dioxide configuration,[16] was taken from Ref. 40. This structure was optimized on a frozen graphene surface at the DFT level with the PBE[41] functional and the D3 correction.[42] Note that throughout this article, we use D3 to refer to the correction with zero-damping, unless stated otherwise. The interaction energy curve configurations were generated by translating the rigid carbon dioxide molecule along the direction perpendicular to graphene. Additional tests on the adsorption configurations are reported in Sec. I of the supplementary material. The adsorption configuration is shown in Fig. 1.

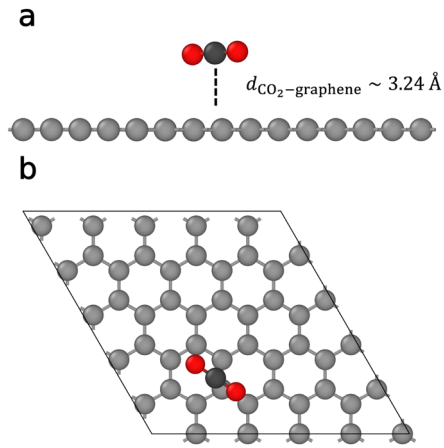

FIG. 1. Adsorption structure of CO_2 on graphene. Top (a) and side (b) views of the adsorption configuration for the CO_2 molecule adsorbed on a graphene sheet. Carbon atoms are shown in gray (with different shades between C atoms belonging to graphene and the C atom in carbon oxide) and oxygen atoms in red.

FN-DMC calculations were performed using CASINO.[43] We use energy-consistent correlated electron pseudopotentials[44] (eCEPP) with the determinant locality approximation[45] (DLA) and the ZSGMA[46] algorithm for the time step convergence. The trial wave-functions were of the Slater–Jastrow type with single Slater determinants, with the single-particle orbitals obtained from DFT local-density approximation (LDA)[47] plane-wave calculations performed with PWscf[48,49] using an energy cutoff of 600 Ry and re-expanded in terms of B-splines.[50] The Jastrow factor includes an electron–electron term, electron–nucleus terms, and electron–electron–nucleus terms. The variational parameters of the Jastrow were optimized by minimizing the variance of the total energy in the adsorbed configuration. We used a DMC time step of 0.01 a.u. and took into account finite size errors (FSE) using the model periodic Coulomb correction[51–53] and further correct for the (smaller) independent particle FSE. We provide additional information on the DMC setup, as well as tests on the convergence of the time step bias and FSE in Secs. S2–S4 of the supplementary material. In addition, we report tests of the sensitivity of the interaction energy estimate to the DFT-optimized structure in Sec. S5 of the supplementary material, showing that the interaction energies obtained for adsorption structures optimized with two different functionals change less than the DMC stochastic error bar.

The interaction energy curves were computed according to Eq. (1), by performing single point calculations (i.e., without geometry optimization). Most DFT calculations of the interaction energy curves were performed with VASP,[54–57] using the projector-augmented plane wave method with hard pseudo-potentials,[58,59] a dense FFT grid, and an energy cutoff of 1000 eV. We use a $1 \times 1 \times 1$ k-point grid to sample the Brillouin zone, except for the hybrid functionals for which we use a $2 \times 2 \times 1$ k-point grid. This

setup provides converged interaction energies to within 1 meV, as shown in Sec. S7 of the supplementary material. The interaction energies with B86bPBE-XDM[60] and the hybrid functionals (PBE0-D3-ATM,[61,62] and B3LYP-D3-ATM,[63,64] where ATM stands for the three body Axilrod–Teller–Muto contribution[65,66]) were computed with FHI-AIMS using the "tight" basis set.[67] The D4-ATM correction was evaluated with the dftd4 package.[68–70] In Sec. S8 of the supplementary material, we show that the VASP and FHI-AIMS setups used in this work yield equivalent level of accuracy on the estimates of the interaction energy. Finally, we evaluated the interaction energies with pre-trained MLIPs using atomistic simulation environment.[71] In the main text, we showcase results for (r^2SCAN[72]-based) MACE-MATPES-r^2SCAN-0 (with the D3 dispersion correction),[73,74] [ωB97M-D3(BJ)[75]-based] MACE-OFF23 (medium),[76] the PBE[41]-based MatterSim (model MatterSim-v1.0.0–5M),[77] and the most recent Universal Models for Atoms (UMA) for molecular crystals (UMA-OMC).[78] Additional models are tested in Sec. S12 of the supplementary material, including the Orb models.[79,80] However, these are not included in the main text because of the size consistency error discussed in Sec. S12.1. Additional details on the DFT calculations, as well as tabulated values of all the DFT interaction energy curves, are provided in Secs. S6, S9, and S11 of the supplementary material.

Figure 2 reports the interaction energy as a function of the CO_2–graphene distance with FN-DMC (red stars) and several DFT approximations. Functionals of similar type are grouped together for comparison. In particular, we report generalized gradient approximation (GGA) functionals (first panel), nonlocal van der Waals (vdW) inclusive functionals (second panel), meta-GGAs (third panel), and hybrids (fourth panel). In addition, we test the performance of a selection of pre-trained MLIPs (fifth panel): MACE-MATPES-r^2SCAN-0 (with the D3 dispersion correction),[73,74] MACE-OFF23,[76] MatterSim,[77] and UMA-OMC.[78] The interaction energy in the adsorbed configuration with a CO_2–graphene distance of ~ 3.24 Å with FN-DMC is -152 ± 15 meV. The adsorption energy computed at the distance ~ 3.33 Å is only slightly higher (-150 ± 13 meV, and equivalent within the stochastic error bar).

We now indicate with ΔE the difference between the DFT and DMC energy in the adsorption configuration with $d \sim 3.24$ Å. The functionals that are in better agreement with DMC are B86bPBE-XDM[60] ($\Delta E \sim 10$ meV), revPBE-D3[42,81] ($\Delta E \sim -12$ meV), PBE-D3[41,42] ($\Delta E \sim -9$ meV), rev-vdW-DF2[82] ($\Delta E \sim -8$ meV), SCAN+rVV10[83] ($\Delta E \sim -11$ meV), and PBE0-D3-ATM ($\Delta E \sim -2$ meV). Note that the energy differences ΔE are all within one standard deviation (15 meV) from the DMC reference value; therefore, these methods are equivalent within the estimated error bar. The plot of the differences between the DFT and DMC prediction is reported in Sec. S10 of the supplementary material.

A highly active area of research in computational materials science is the development of foundation machine learning force fields, which aim to enable DFT-level accuracy simulation of large and realistic systems at a fraction of the computational cost. In this context, benchmarking their performance against high-level reference data is valuable to assess their suitability for modeling extended systems and prototypical device architectures. In particular, we find that the interaction energy at the minimum is well-reproduced with MACE-OFF23 and UMA-OMC. Additional data on the performance of the pre-trained models is reported in Sec. S12 of the supplementary material.

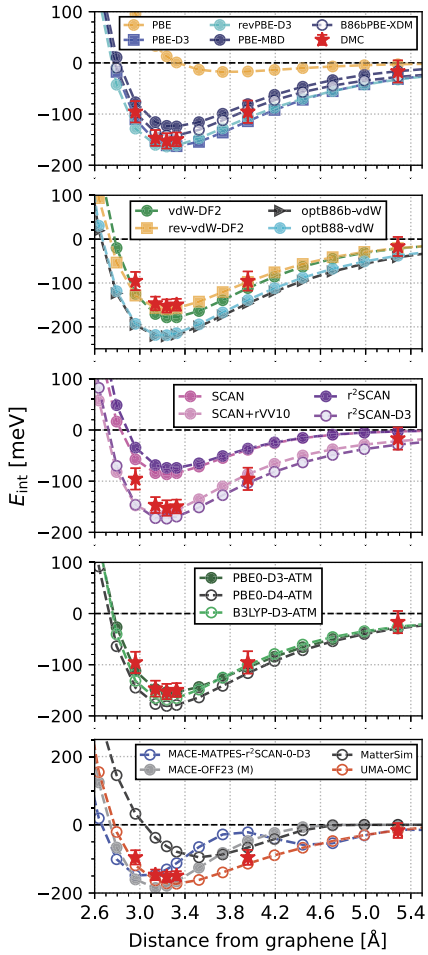

FIG. 2. Interaction energy curves of carbon dioxide on graphene. The figure shows the interaction energy as a function of the carbon dioxide–graphene distance with reference DMC calculation (red stars) and several density functional approximations (GGA first panel, non-local vdW functionals second panel, meta-GGA third panel, and hybrids fourth panel), and machine learning force fields (fifth panel). Here, M stands for "medium" model.

A value of ~−213 meV has been reported with SAPT calculations for the carbon dioxide–graphene interaction energy. This value was computed with SAPT0 on PBE-D3 optimized geometries via cluster expansion extrapolation, with the jun-cc-pVDZ basis set.[16] The interaction energy reported in our work is higher than both the experimental estimates and the SAPT0 prediction. The difference with the experiment is expected due to the influence of the substrate on the adsorption energy and structure.[14–16] As shown in Ref. 16 with PBE-D3 calculations, cluster extrapolated estimates tend to overbind the interaction energy by ~10 – 20 meV. The methodological differences between the cluster extrapolated SAPT0 and periodic FN-DMC might further contribute to the discrepancy between the two theoretical predictions.

So far, we have focused on the adsorption of carbon dioxide on graphene. However, carbon capture technologies may depend on the competitive adsorption between carbon dioxide and water molecules.[37–39] It is not clear *a priori* which molecule is likely to interact more strongly with the substrate. Therefore, in Fig. 3, we investigate such competitive adsorption by comparing the interaction energy in the adsorbed configuration computed with FN-DMC and DFT, both for the CO_2 molecule (red) and the water molecule (blue).

The reference FN-DMC value for the interaction energy of a single water molecule on free-standing graphene is $E_{\rm int}^{\rm H_2O} = -99 \pm 6$ meV. This was computed for the "2-leg" water configuration, that is, with both hydrogen atoms pointing toward graphene, using the same setup as in Eq. (1).[24] The DFT interaction energies for the water molecule were taken from Ref. 84, except for the functionals B86bPBE-XDM, r^{2}SCAN, r^{2}SCAN-D3, PBE0-D3-ATM, PBE0-D4-ATM, and B3LYP-D3-ATM computed in this work. Details of the water–graphene calculations are provided in Sec. S11. FN-DMC predicts that CO_2 binds more strongly than water to pristine graphene, with a difference of $E_{\rm int}^{\rm CO_2} - E_{\rm int}^{\rm H_2O}$ of $\sim -53 \pm 16$ meV. Most of the tested approximations qualitatively capture this trend, except for PBE, PBE-MBD, SCAN, and r^{2}SCAN. Quantitatively, the closest agreement for the interaction energy difference between carbon dioxide and water is obtained with vdW-DF2,[85] rev-vdW-DF2,[82] and PBE0-D4-ATM. Interestingly, all the functionals tested in this work except the non-local vdW functionals and PBE0-D4-ATM underestimate the interaction energy difference. A plot of the difference between the DFT and DMC on the relative interaction energy $E_{\rm int}^{\rm CO_2} - E_{\rm int}^{\rm H_2O}$ is reported in Sec. S10 of the supplementary material. Among the tested MLIPs, MACE-OFF23 is the most reliable, yielding $E_{\rm int}^{\rm CO_2} - E_{\rm int}^{\rm H_2O} \sim -58$ meV, followed by UMA-OMC, which predicts $E_{\rm int}^{\rm CO_2} - E_{\rm int}^{\rm H_2O} \sim 0.1$ meV. However, this value is sensitive to the ~25 meV size consistency error discussed in the supplementary material. By contrast, MatterSim underbinds the water molecule and predicts $E_{\rm int}^{\rm CO_2} - E_{\rm int}^{\rm H_2O} \sim -147$ meV, while MACE-MATPES-r2SCAN-D3 significantly overbinds the water molecule by predicting $E_{\rm int}^{\rm CO_2} - E_{\rm int}^{\rm H_2O} \sim 548$ meV.

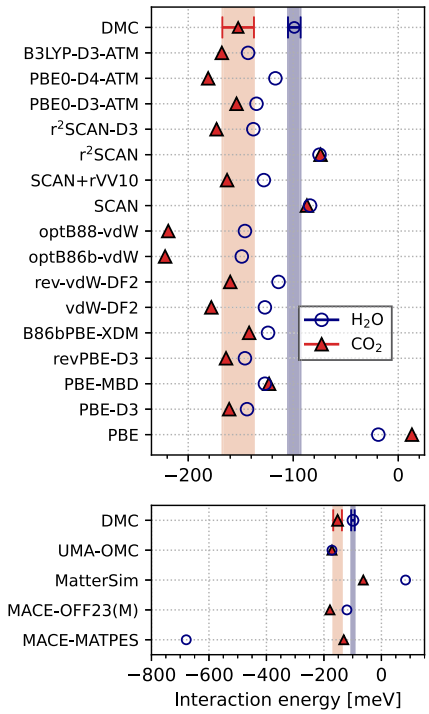

FIG. 3. Interaction strength of carbon dioxide and water on graphene. The figure shows the interaction energy (in meV) with DMC (first row of each panel), DFT (top panel), and machine learning force fields (bottom panel) for carbon dioxide on graphene (in the adsorbed configuration at $d \sim 3.24$ Å, red triangles) and the water molecule on graphene (blue empty circles). The shaded areas highlight the stochastic error bar on the DMC calculations. The DMC reference energy for the water molecule adsorbed on graphene is taken from Ref. 24. "MACE-MATPES" stands for MACE-MATPES-r^{2}SCAN-0-D3.

Finally, we comment on the nature of the carbon dioxide–graphene interaction. By analyzing the electronic charge rearrangement upon adsorption, Brandenburg *et al.*[24] showed that although the water–graphene interaction is mainly dominated by dispersion effects, electrostatics play a significant role depending on the different orientations of the hydrogen atoms with respect to graphene. In Fig. 4, we compare the change of electronic charge density upon adsorption of both carbon dioxide and water on graphene. In particular, we plot the top and side views of the charge density rearrangement for water (left) and carbon dioxide (right) adsorbed on graphene. The charge densities were computed with VASP with PBE-D3 and plotted with VESTA.[86] The plot shows that the charge redistribution is much more localized for the CO_2 molecule compared to the water molecule. Therefore, as suggested from both Figs. 2 and 3, dispersion is the main interaction characterizing the adsorption of carbon dioxide on graphene. As pointed out in Ref. 24, differences in the charge density rearrangement lead to a variation in the surface multipole moment and hence the work function of the substrate, which can in principle be observed in experiment.

In summary, we provide FN-DMC interaction energy curves for carbon dioxide on a periodic graphene sheet and used these to evaluate the performance of several DFT functionals and MLIPs. The reference interaction energy obtained in this work is -152 ± 15 meV, which means that a CO_2 molecule binds $\sim 53 \pm 16$ meV stronger than a water molecule on graphene. Among the tested foundation MLIPs, MACE-OFF23 and UMA-OMC yield the closest agreement for the interaction energy in the adsorbed configuration. The B86bPBE-XDM, PBE-D3, revPBE-D3, rev-vdW-DF2, SCAN+rVV10, r^{2}SCAN-D3, and PBE0-D3-ATM functionals yield the closest agreement with FN-DMC for the interaction energy of CO_2 on graphene. Interestingly, vdW-DF2, rev-vdW-DF2, and PBE0-D4-ATM obtain the closest agreement for the difference between the interaction energy of carbon dioxide and water on graphene. Overall, the FN-DMC interaction energies computed in this work provide useful reference values for benchmarks of electronic structure approaches and could be further used for parameterization of analytical potentials.

The supplementary material provides additional information on the setup and convergence tests of both DMC and DFT

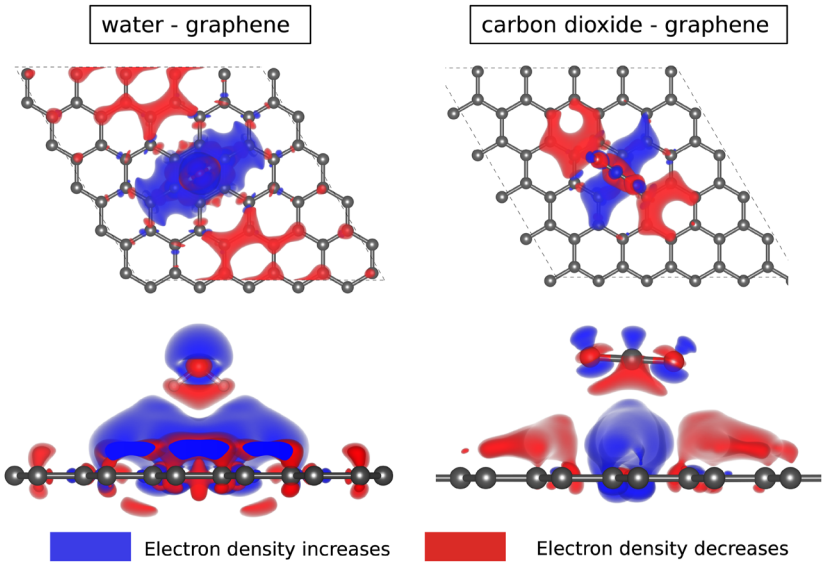

FIG. 4. Electronic density rearrangement upon adsorption. The figure shows the difference between the electronic density of the adsorbed configuration and each individual fragments, for water (left) and carbon dioxide (right). For each system, we report the top and side views of the charge density isosurfaces. The isosurface level is 7.10855 $\times 10^{-5}$ electrons/Å^3. The unit cell is indicated by the black dashed lines. The blue regions indicate density increase upon binding and the red regions indicate depletion.

simulations; additional information on the benchmark of DFT functionals for the carbon dioxide–graphene and water–graphene interaction energies; tabulated values of the interaction energy curves for all the DFT approximations considered in this work; additional information on the performance of pre-trained MLIPs; and additional tests on the adsorption structure and the influence of the DFT-optimized structure on the estimate of the interaction energy. The supplementary material contains Refs. 16, 24, 32, 40–46, 48–67, 72, 75, 76, and 78–95.

This work used the ARCHER2 UK National Supercomputing Service (https://www.archer2.ac.uk), for which access was funded by EPSRC under Grant No. HPC/APP37347. This work was also performed using resources provided by the Cambridge Service for Data Driven Discovery (CSD3) operated by the University of Cambridge Research Computing Service (www.csd3.cam.ac.uk), provided by Dell EMC and Intel using Tier-2 funding from the Engineering and Physical Sciences Research Council (capital Grant Nos. EP/T022159/1 and EP/P020259/1), and DiRAC funding from the Science and Technology Facilities Council (www.dirac.ac.uk). A.M. acknowledges support from the European Union under the "n-AQUA" European Research Council project (Grant No. 101071937). F.B. acknowledges support from the Alexander von Humboldt Foundation through a Feodor Lynen Research Fellowship, from the Isaac Newton Trust through an Early Career Fellowship, and from Churchill College, Cambridge, through a Postdoctoral By-Fellowship. A.Z. and D.A. acknowledge support from the European Union under the Next Generation EU (Project Nos. 20222FXZ33 and P2022MC742).

AUTHOR DECLARATIONS

Conflict of Interest

The authors have no conflicts to disclose.

Author Contributions

Flaviano Della Pia: Conceptualization (equal); Data curation (lead); Formal analysis (equal); Writing – original draft (lead); Writing – review & editing (equal). **Giaan Kler-Young**: Conceptualization (equal); Data curation (equal); Formal analysis (equal); Writing – review & editing (equal). **Andrea Zen**: Conceptualization (equal); Data curation (equal); Formal analysis (equal); Resources (lead); Supervision (equal); Writing – review & editing (equal). **Fabian Berger**: Conceptualization (equal); Data curation (equal); Formal analysis (equal); Supervision (equal); Writing – review & editing (equal). **Dario Alfè**: Conceptualization (equal); Data curation (equal); Formal analysis (equal); Resources (lead); Supervision (equal); Writing – review & editing (equal). **Angelos Michaelides**: Conceptualization (equal); Data curation (equal); Formal analysis (equal); Project administration (lead); Resources (lead); Supervision (lead); Writing – review & editing (equal).

DATA AVAILABILITY

All the data necessary to reproduce the findings of this work are provided in the paper and its supplementary material. Scripts as well as input and output files are provided on GitHub.

REFERENCES

[1] X. Liu, D. Lyu, C. Merlet, M. J. A. Leesmith, X. Hua, Z. Xu, C. P. Grey, and A. C. Forse, "Structural disorder determines capacitance in nanoporous carbons," Science **384**, 321–325 (2024).
[2] X. Liu, R. Hunter, Z. Xu, E. H. Lahrar, C. Merlet, C. Grey, M.-M. Titirici, and A. Forse, "Highly disordered nanoporous carbons for enhanced energy storage in supercapacitors," chemRxiv:chemrxiv-2025-4wvlj (2025).
[3] F. Schedin, A. K. Geim, S. V. Morozov, E. W. Hill, P. Blake, M. I. Katsnelson, and K. S. Novoselov, "Detection of individual gas molecules adsorbed on graphene," Nat. Mater. **6**, 652–655 (2007).

[4]Y. Shao, J. Wang, H. Wu, J. Liu, I. Aksay, and Y. Lin, "Graphene based electrochemical sensors and biosensors: A review," Electroanalysis **22**, 1027–1036 (2010).
[5]J. H. Choi, J. Lee, M. Byeon, T. E. Hong, H. Park, and C. Y. Lee, "Graphene-based gas sensors with high sensitivity and minimal sensor-to-sensor variation," ACS Appl. Nano Mater. **3**, 2257–2265 (2020).
[6]E. Singh, M. Meyyappan, and H. S. Nalwa, "Flexible graphene-based wearable gas and chemical sensors," ACS Appl. Mater. Interfaces **9**, 34544–34586 (2017).
[7]A. Piras, C. Ehlert, and G. Gryn'ova, "Sensing and sensitivity: Computational chemistry of graphene-based sensors," WIREs Comput. Mol. Sci. **11**, e1526 (2021).
[8]N. A. Hartley, Z. Xu, T. Kress, and A. C. Forse, "Correlating the structure of quinone-functionalized carbons with electrochemical CO_2 capture performance," Mater. Today Energy **45**, 101689 (2024).
[9]H. Li, M. E. Zick, T. Trisukhon, M. Signorile, X. Liu, H. Eastmond, S. Sharma, T. L. Spreng, J. Taylor, J. W. Gittins, C. Farrow, S. A. Lim, V. Crocellà, P. J. Milner, and A. C. Forse, "Capturing carbon dioxide from air with charged-sorbents," Nature **630**, 654–659 (2024).
[10]G. Mapstone, T. M. Kamsma, Z. Xu, P. K. Jones, A. A. Lee, I. Temprano, J. Lee, M. F. L. De Volder, and A. C. Forse, "Understanding the mechanism of electrochemical CO_2 capture by supercapacitive swing adsorption," ACS Nano **19**, 4242–4250 (2025).
[11]T. K. Junita, N. Syakir, F. Faizal, and Fitrilawati, "Graphene-based composite for carbon capture," ACS Omega **9**, 20658–20669 (2024).
[12]Z. Xu, X. Liu, G. Mapstone, Z. Coady, C. Seymour, S. E. Wiesner, S. Menkin, and A. C. Forse, "Breaking supercapacitor symmetry enhances electrochemical carbon dioxide capture," J. Am. Chem. Soc. **147**, 16189 (2025).
[13]Z. Xu, G. Mapstone, Z. Coady, M. Wang, T. L. Spreng, X. Liu, D. Molino, and A. C. Forse, "Enhancing electrochemical carbon dioxide capture with supercapacitors," Nat. Commun. **15**, 7851 (2024).
[14]K. Takeuchi, S. Yamamoto, Y. Hamamoto, Y. Shiozawa, K. Tashima, H. Fukidome, T. Koitaya, K. Mukai, S. Yoshimoto, M. Suemitsu, Y. Morikawa, J. Yoshinobu, and I. Matsuda, "Adsorption of CO_2 on graphene: A combined TPD, XPS, and vdW-DF study," J. Phys. Chem. C **121**, 2807–2814 (2017).
[15]R. S. Smith and B. D. Kay, "Desorption kinetics of carbon dioxide from a graphene-covered pt(111) surface," J. Phys. Chem. A **123**, 3248–3254 (2019).
[16]C. Ehlert, A. Piras, and G. Gryn'ova, "CO_2 on graphene: Benchmarking computational approaches to noncovalent interactions," ACS Omega **8**, 35768–35778 (2023).
[17]M. Stachová, M. Dubecký, and F. Karlický, "Adsorption of atomic and molecular monolayers on pt-supported graphene," Chem. Phys. **564**, 111713 (2023).
[18]P. Lazar, F. Karlický, P. Jurečka, M. Kocman, E. Otyepková, K. Šafářová, and M. Otyepka, "Adsorption of small organic molecules on graphene," J. Am. Chem. Soc. **135**, 6372–6377 (2013).
[19]B. X. Shi, A. Zen, V. Kapil, P. R. Nagy, A. Grüneis, and A. Michaelides, "Many-body methods for surface chemistry come of age: Achieving consensus with experiments," J. Am. Chem. Soc. **145**, 25372–25381 (2023).
[20]Y. S. Al-Hamdani, M. Ma, D. Alfè, O. A. von Lilienfeld, and A. Michaelides, "Communication: Water on hexagonal boron nitride from diffusion Monte Carlo," J. Chem. Phys. **142**, 181101 (2015).
[21]Y. S. Al-Hamdani, D. Alfè, and A. Michaelides, "How strongly do hydrogen and water molecules stick to carbon nanomaterials?," J. Chem. Phys. **146**, 094701 (2017).
[22]Y. S. Al-Hamdani, M. Rossi, D. Alfè, T. Tsatsoulis, B. Ramberger, J. G. Brandenburg, A. Zen, G. Kresse, A. Grüneis, A. Tkatchenko, and A. Michaelides, "Properties of the water to boron nitride interaction: From zero to two dimensions with benchmark accuracy," J. Chem. Phys. **147**, 044710 (2017).
[23]J. G. Brandenburg, A. Zen, D. Alfè, and A. Michaelides, "Interaction between water and carbon nanostructures: How good are current density functional approximations?," J. Chem. Phys. **151**, 164702 (2019).
[24]J. G. Brandenburg, A. Zen, M. Fitzner, B. Ramberger, G. Kresse, T. Tsatsoulis, A. Grüneis, A. Michaelides, and D. Alfè, "Physisorption of water on graphene: Subchemical accuracy from many-body electronic structure methods," J. Phys. Chem. Lett. **10**, 358–368 (2019).
[25]T. Tsatsoulis, F. Hummel, D. Usvyat, M. Schütz, G. H. Booth, S. S. Binnie, M. J. Gillan, D. Alfè, A. Michaelides, and A. Grüneis, "A comparison between quantum chemistry and quantum Monte Carlo techniques for the adsorption of water on the (001) LiH surface," J. Chem. Phys. **146**, 204108 (2017).
[26]C.-R. Hsing, C.-M. Chang, C. Cheng, and C.-M. Wei, "Quantum Monte Carlo studies of co adsorption on transition metal surfaces," J. Phys. Chem. C **123**, 15659–15664 (2019).
[27]A. D. Powell, N. Gerrits, T. Tchakoua, M. F. Somers, H. F. Busnengo, J. Meyer, G.-J. Kroes, and K. Doblhoff-Dier, "Best-of-both-worlds predictive approach to dissociative chemisorption on metals," J. Phys. Chem. Lett. **15**, 307–315 (2024).
[28]R. Fanta and M. Bajdich, "Resolution of selectivity steps of CO reduction reaction on copper by quantum Monte Carlo," J. Phys. Chem. Lett. **16**, 1494–1500 (2025).
[29]Y. S. Al-Hamdani, A. Zen, and D. Alfè, "Unraveling H_2 chemisorption and physisorption on metal decorated graphene using quantum Monte Carlo," J. Chem. Phys. **159**(20), 204708 (2023).
[30]F. Della Pia, A. Zen, D. Alfè, and A. Michaelides, "DMC-ICE13: Ambient and high pressure polymorphs of ice from diffusion Monte Carlo and density functional theory," J. Chem. Phys. **157**, 134701 (2022).
[31]F. Della Pia, A. Zen, D. Alfè, and A. Michaelides, "How accurate are simulations and experiments for the lattice energies of molecular crystals?," Phys. Rev. Lett. **133**, 046401 (2024).
[32]A. Zen, J. G. Brandenburg, J. Klimeš, A. Tkatchenko, D. Alfè, and A. Michaelides, "Fast and accurate quantum Monte Carlo for molecular crystals," Proc. Natl. Acad. Sci. U. S. A. **115**, 1724–1729 (2018).
[33]B. X. Shi, F. D. Pia, Y. S. Al-Hamdani, A. Michaelides, D. Alfè, and A. Zen, "Systematic discrepancies between reference methods for noncovalent interactions within the S66 dataset," J. Chem. Phys. **162**, 144107 (2025).
[34]F. Della Pia, B. Shi, Y. S. Al-Hamdani, D. Alfè, T. Anderson, M. Barborini, A. Benali, M. Casula, N. Drummond, M. Dubecký, C. Filippi, P. Kent, J. Krogel, P. L. Rios, A. Lüchow, Y. Luo, A. Michaelides, L. Mitas, K. Nakano, R. Needs, M. Per, A. Scemama, J. Schultze, R. Shinde, E. Slootman, S. Sorella, A. Tkatchenko, M. Towler, C. Umrigar, L. Wagner, W. A. Wheeler, H. Zhou, and A. Zen, "Is fixed-node diffusion quantum Monte Carlo reproducible?," arXiv:2501.12950 (2025).
[35]M. Dubecký, R. Derian, P. Jurečka, L. Mitas, P. Hobza, and M. Otyepka, "Quantum Monte Carlo for noncovalent interactions: An efficient protocol attaining benchmark accuracy," Phys. Chem. Chem. Phys. **16**, 20915–20923 (2014).
[36]M. He, H. Zhao, X. Yang, J. Jia, X. Liu, Z. Qu, W. Zhou, F. Sun, and Z. Wang, "Reconsideration about the competitive adsorption of H_2O and CO_2 on carbon surfaces: The influence of oxygen functional groups," J. Environ. Chem. Eng. **11**, 111288 (2023).
[37]P. G. Boyd, A. Chidambaram, E. García-Díez, C. P. Ireland, T. D. Daff, R. Bounds, A. Gładysiak, P. Schouwink, S. M. Moosavi, M. M. Maroto-Valer, J. A. Reimer, J. A. R. Navarro, T. K. Woo, S. Garcia, K. C. Stylianou, and B. Smit, "Data-driven design of metal–organic frameworks for wet flue gas CO_2 capture," Nature **576**, 253–256 (2019).
[38]C.-H. Ho and F. Paesani, "Elucidating the competitive adsorption of H_2O and CO_2 in CALF-20: New insights for enhanced carbon capture metal–organic frameworks," ACS Appl. Mater. Interfaces **15**, 48287–48295 (2023).
[39]T. T. T. Nguyen, B. M. Balasubramaniam, N. Fylstra, R. P. S. Huynh, G. K. H. Shimizu, and A. Rajendran, "Competitive CO_2/H_2O adsorption on CALF-20," Ind. Eng. Chem. Res. **63**, 3265–3281 (2024).
[40]I. C. Popoola, B. X. Shi, F. Berger, A. Michaelides, A. Zen, D. Alfè, and Y. S. Al-Hamdani, "Cooperative CO_2 capture via oxalate formation on metal-decorated graphene," Phys. Rev. Mater. **9**, 015401 (2025).
[41]J. P. Perdew, K. Burke, and M. Ernzerhof, "Generalized gradient approximation made simple," Phys. Rev. Lett. **77**, 3865–3868 (1996).
[42]S. Grimme, J. Antony, S. Ehrlich, and H. Krieg, "A consistent and accurate *ab initio* parametrization of density functional dispersion correction (DFT-D) for the 94 elements H-Pu," J. Chem. Phys. **132**, 154104 (2010).
[43]R. J. Needs, M. D. Towler, N. D. Drummond, P. López Ríos, and J. R. Trail, "Variational and diffusion quantum Monte Carlo calculations with the CASINO code," J. Chem. Phys. **152**, 154106 (2020).
[44]J. R. Trail and R. J. Needs, "Shape and energy consistent pseudopotentials for correlated electron systems," J. Chem. Phys. **146**, 204107 (2017).

[45] A. Zen, J. G. Brandenburg, A. Michaelides, and D. Alfè, "A new scheme for fixed node diffusion quantum Monte Carlo with pseudopotentials: Improving reproducibility and reducing the trial-wave-function bias," J. Chem. Phys. **151**, 134105 (2019).
[46] A. Zen, S. Sorella, M. J. Gillan, A. Michaelides, and D. Alfè, "Boosting the accuracy and speed of quantum Monte Carlo: Size consistency and time step," Phys. Rev. B **93**, 241118 (2016).
[47] J. P. Perdew and A. Zunger, "Self-interaction correction to density-functional approximations for many-electron systems," Phys. Rev. B **23**, 5048–5079 (1981).
[48] Quantum espresso http://www.quantum-espresso.org./.
[49] Pwscf http://www.pwscf.org./.
[50] D. Alfè and M. J. Gillan, "Efficient localized basis set for quantum Monte Carlo calculations on condensed matter," Phys. Rev. B **70**, 161101 (2004).
[51] L. M. Fraser, W. M. C. Foulkes, G. Rajagopal, R. J. Needs, S. D. Kenny, and A. J. Williamson, "Finite-size effects and Coulomb interactions in quantum Monte Carlo calculations for homogeneous systems with periodic boundary conditions," Phys. Rev. B **53**, 1814–1832 (1996).
[52] A. J. Williamson, G. Rajagopal, R. J. Needs, L. M. Fraser, W. M. C. Foulkes, Y. Wang, and M.-Y. Chou, "Elimination of Coulomb finite-size effects in quantum many-body simulations," Phys. Rev. B **55**, R4851 (1997).
[53] P. R. C. Kent, R. Q. Hood, A. J. Williamson, R. J. Needs, W. M. C. Foulkes, and G. Rajagopal, "Finite-size errors in quantum many-body simulations of extended systems," Phys. Rev. B **59**, 1917–1929 (1999).
[54] G. Kresse and J. Hafner, "*Ab initio* molecular dynamics for liquid metals," Phys. Rev. B **47**, 558 (1993).
[55] G. Kresse and J. Hafner, "*Ab initio* molecular-dynamics simulation of the liquid-metal–amorphous-semiconductor transition in germanium," Phys. Rev. B **49**, 14251 (1994).
[56] G. Kresse and J. Furthmüller, "Efficiency of ab-initio total energy calculations for metals and semiconductors using a plane-wave basis set," Comput. Mater. Sci. **6**, 15–50 (1996).
[57] G. Kresse and J. Furthmüller, "Efficient iterative schemes for *ab initio* total-energy calculations using a plane-wave basis set," Phys. Rev. B **54**, 11169 (1996).
[58] G. Kresse and D. Joubert, "From ultrasoft pseudopotentials to the projector augmented-wave method," Phys. Rev. B **59**, 1758 (1999).
[59] P. E. Blöchl, "Projector augmented-wave method," Phys. Rev. B **50**, 17953 (1994).
[60] A. J. A. Price, A. Otero-de-la Roza, and E. R. Johnson, "XDM-corrected hybrid DFT with numerical atomic orbitals predicts molecular crystal lattice energies with unprecedented accuracy," Chem. Sci. **14**, 1252–1262 (2023).
[61] J. P. Perdew, M. Ernzerhof, and K. Burke, "Rationale for mixing exact exchange with density functional approximations," J. Chem. Phys. **105**, 9982–9985 (1996).
[62] C. Adamo and V. Barone, "Toward reliable density functional methods without adjustable parameters: The PBE0 model," J. Chem. Phys. **110**, 6158–6170 (1999).
[63] A. D. Becke, "Density-functional thermochemistry. III. The role of exact exchange," J. Chem. Phys. **98**, 5648–5652 (1993).
[64] C. Lee, W. Yang, and R. G. Parr, "Development of the Colle–Salvetti correlation-energy formula into a functional of the electron density," Phys. Rev. B **37**, 785–789 (1988).
[65] B. M. Axilrod and E. Teller, "Interaction of the van der waals type between three atoms," J. Chem. Phys. **11**, 299–300 (1943).
[66] Y. Muto, "Force between nonpolar molecules," Proc. Phys.-Math. Soc. Jpn. **17**, 629–631 (1943).
[67] V. Blum, R. Gehrke, F. Hanke, P. Havu, V. Havu, X. Ren, K. Reuter, and M. Scheffler, "*Ab initio* molecular simulations with numeric atom-centered orbitals," Comput. Phys. Commun. **180**, 2175–2196 (2009).
[68] E. Caldeweyher, C. Bannwarth, and S. Grimme, "Extension of the D3 dispersion coefficient model," J. Chem. Phys. **147**, 034112 (2017).
[69] E. Caldeweyher, S. Ehlert, A. Hansen, H. Neugebauer, S. Spicher, C. Bannwarth, and S. Grimme, "A generally applicable atomic-charge dependent London dispersion correction," J. Chem. Phys. **150**, 154122 (2019).
[70] E. Caldeweyher, J.-M. Mewes, S. Ehlert, and S. Grimme, "Extension and evaluation of the D4 London-dispersion model for periodic systems," Phys. Chem. Chem. Phys. **22**, 8499–8512 (2020).
[71] A. Hjorth Larsen, J. Jørgen Mortensen, J. Blomqvist, I. E. Castelli, R. Christensen, M. Dułak, J. Friis, M. N. Groves, B. Hammer, C. Hargus, E. D. Hermes, P. C. Jennings, P. Bjerre Jensen, J. Kermode, J. R. Kitchin, E. Leonhard Kolsbjerg, J. Kubal, K. Kaasbjerg, S. Lysgaard, J. Bergmann Maronsson, T. Maxson, T. Olsen, L. Pastewka, A. Peterson, C. Rostgaard, J. Schiøtz, O. Schütt, M. Strange, K. S. Thygesen, T. Vegge, L. Vilhelmsen, M. Walter, Z. Zeng, and K. W. Jacobsen, "The atomic simulation environment—A Python library for working with atoms," J. Phys.: Condens. Matter **29**, 273002 (2017).
[72] J. W. Furness, A. D. Kaplan, J. Ning, J. P. Perdew, and J. Sun, "Accurate and numerically efficient r^2SCAN meta-generalized gradient approximation," J. Phys. Chem. Lett. **11**, 8208–8215 (2020).
[73] I. Batatia, P. Benner, Y. Chiang, A. M. Elena, D. P. Kovács, J. Riebesell, X. R. Advincula, M. Asta, W. J. Baldwin, N. Bernstein, A. Bhowmik, S. M. Blau, V. Cărare, J. P. Darby, S. De, F. D. Pia, V. L. Deringer, R. Elijošius, Z. El-Machachi, E. Fako, A. C. Ferrari, A. Genreith-Schriever, J. George, R. E. A. Goodall, C. P. Grey, S. Han, W. Handley, H. H. Heenen, K. Hermansson, C. Holm, J. Jaafar, S. Hofmann, K. S. Jakob, H. Jung, V. Kapil, A. D. Kaplan, N. Karimitari, N. Kroupa, J. Kullgren, M. C. Kuner, D. Kuryla, G. Liepuoniute, J. T. Margraf, I.-B. Magdău, A. Michaelides, J. H. Moore, A. A. Naik, S. P. Niblett, S. W. Norwood, N. O'Neill, C. Ortner, K. A. Persson, K. Reuter, A. S. Rosen, L. L. Schaaf, C. Schran, E. Sivonxay, T. K. Stenczel, V. Svahn, C. Sutton, C. van der Oord, E. Varga-Umbrich, T. Vegge, M. Vondrák, Y. Wang, W. C. Witt, F. Zills, and G. Csányi, "A foundation model for atomistic materials chemistry," arXiv:2401.00096 (2023).
[74] A. D. Kaplan, R. Liu, J. Qi, T. W. Ko, B. Deng, J. Riebesell, G. Ceder, K. A. Persson, and S. P. Ong, "A foundational potential energy surface dataset for materials," arXiv:2503.04070 (2025).
[75] N. Mardirossian and M. Head-Gordon, "ωB97X-V: A 10-parameter, range-separated hybrid, generalized gradient approximation density functional with nonlocal correlation, designed by a survival-of-the-fittest strategy," Phys. Chem. Chem. Phys. **16**, 9904–9924 (2014).
[76] D. P. Kovács, J. H. Moore, N. J. Browning, I. Batatia, J. T. Horton, V. Kapil, Y. Pu, W. C. Witt, I.-B. Magdău, D. J. Cole, and G. Csányi, "MACE-OFF: Transferable machine learning force fields for organic molecules," J. Am. Chem. Soc. **147**(21), 17598–17611 (2025).
[77] H. Yang, C. Hu, Y. Zhou, X. Liu, Y. Shi, J. Li, G. Li, Z. Chen, S. Chen, C. Zeni, M. Horton, R. Pinsler, A. Fowler, D. Zügner, T. Xie, J. Smith, L. Sun, Q. Wang, L. Kong, C. Liu, H. Hao, and Z. Lu, "MatterSim: A deep learning atomistic model across elements, temperatures and pressures," arXiv:2405.04967 (2024).
[78] D. S. Levine, M. Shuaibi, E. W. C. Spotte-Smith, M. G. Taylor, M. R. Hasyim, K. Michel, I. Batatia, G. Csányi, M. Dzamba, P. Eastman, N. C. Frey, X. Fu, V. Gharakhanyan, A. S. Krishnapriyan, J. A. Rackers, S. Raja, A. Rizvi, A. S. Rosen, Z. Ulissi, S. Vargas, C. L. Zitnick, S. M. Blau, and B. M. Wood, "The open molecules 2025 (OMol25) dataset, evaluations, and models," arXiv:2505.08762 [physics.chem-ph] (2025).
[79] M. Neumann, J. Gin, B. Rhodes, S. Bennett, Z. Li, H. Choubisa, A. Hussey, and J. Godwin, "Orb: A fast, scalable neural network potential," arXiv:2410.22570 (2024).
[80] B. Rhodes, S. Vandenhaute, V. Šimkus, J. Gin, J. Godwin, T. Duignan, and M. Neumann, "Orb-v3: Atomistic simulation at scale," arXiv:2504.06231 (2025).
[81] Y. Zhang and W. Yang, "Comment on 'generalized gradient approximation made simple,'" Phys. Rev. Lett. **80**, 890 (1998).
[82] I. Hamada, "van der Waals density functional made accurate," Phys. Rev. B **89**, 121103 (2014).
[83] H. Peng, Z.-H. Yang, J. P. Perdew, and J. Sun, "Versatile van der Waals density functional based on a meta-generalized gradient approximation," Phys. Rev. X **6**, 041005 (2016).
[84] F. Della Pia, A. Zen, V. Kapil, F. L. Thiemann, D. Alfè, and A. Michaelides, "On the increase of the melting temperature of water confined in one-dimensional nano-cavities," J. Chem. Phys. **161**, 224706 (2024).
[85] K. Lee, É. D. Murray, L. Kong, B. I. Lundqvist, and D. C. Langreth, "Higher-accuracy van der Waals density functional," Phys. Rev. B **82**, 081101 (2010).
[86] K. Momma and F. Izumi, "*VESTA 3* for three-dimensional visualization of crystal, volumetric and morphology data," J. Appl. Crystallogr. **44**, 1272–1276 (2011).

[87] W. M. C. Foulkes, L. Mitas, R. J. Needs, and G. Rajagopal, "Quantum Monte Carlo simulations of solids," Rev. Mod. Phys. **73**, 33–83 (2001).
[88] A. Tkatchenko, R. A. DiStasio, R. Car, and M. Scheffler, "Accurate and efficient method for many-body van der Waals interactions," Phys. Rev. Lett. **108**, 236402 (2012).
[89] A. Ambrosetti, A. M. Reilly, R. A. DiStasio, and A. Tkatchenko, "Long-range correlation energy calculated from coupled atomic response functions," J. Chem. Phys. **140**, 18A508 (2014).
[90] J. Klimeš, D. R. Bowler, and A. Michaelides, "Van der Waals density functionals applied to solids," Phys. Rev. B **83**, 195131 (2011).
[91] J. Klimeš, D. R. Bowler, and A. Michaelides, "Chemical accuracy for the van der Waals density functional," J. Phys.: Condens. Matter **22**, 022201 (2009).
[92] J. Sun, A. Ruzsinszky, and J. P. Perdew, "Strongly constrained and appropriately normed semilocal density functional," Phys. Rev. Lett. **115**, 036402 (2015).
[93] S. Ehlert, U. Huniar, J. Ning, J. W. Furness, J. Sun, A. D. Kaplan, J. P. Perdew, and J. G. Brandenburg, "r^2SCAN-D4: Dispersion corrected meta-generalized gradient approximation for general chemical applications," J. Chem. Phys. **154**, 061101 (2021).
[94] J. Schmidt, T. F. T. Cerqueira, A. H. Romero, A. Loew, F. Jäger, H.-C. Wang, S. Botti, and M. A. L. Marques, "Improving machine-learning models in materials science through large datasets," Mater. Today Phys. **48**, 101560 (2024).
[95] L. Barroso-Luque, M. Shuaibi, X. Fu, B. M. Wood, M. Dzamba, M. Gao, A. Rizvi, C. L. Zitnick, and Z. W. Ulissi, "Open materials 2024 (OMat24) inorganic materials dataset and models," arXiv:2410.12771 (2024).